High-pressure Raman scattering and structural phase transition in $YCrO_4$

Y. W. Long, L. X. Yang, Y. Yu, F. Y. Li, R. C. Yu, S. Ding, Y. L. Liu, and C. Q. Jin*
National Lab for Condensed Matter Physics, Institute of Physics, Chinese Academy of Sciences, Beijing 100080, People's Republic of China

(Received 11 April 2006; revised manuscript received 18 June 2006; published 23 August 2006)

The high-pressure structural properties of the zircon-type $YCrO_4$ with space group $I4_1/amd$ were investigated using Raman scattering techniques in a diamond anvil cell up to 28.9 GPa at room temperature. The abrupt changes in Raman spectra indicate that a pressure-induced structural phase transition occurs at a lower pressure 3.0 GPa, but a wide pressure region up to 15.1 GPa is needed to complete this phase transition. Moreover, the high-pressure phase can be quenched at ambient conditions. We calculated the mode Grüneisen parameters and assigned the new phase to be a scheelite-type structure in $I4_1/a$ symmetry based on the fact that the Raman spectrum of the new phase is similar to that of the scheelite-type $YCrO_4$ prepared at moderate pressure and temperature conditions. The effects of $3d^1$ electronic configuration on phase transition pressure and unusual Raman vibrations were discussed.

DOI: 10.1103/PhysRevB.74.054110 PACS number(s): 61.50.Ks, 62.50.+p, 33.20.Fb

I. INTRODUCTION

Zircon- and scheelite-type compounds with the chemical composition ABX_4 are kinds of attractive materials in theoretical studies as well as in applied realms related to solid-state scintillators, laser host materials, and optoelectronic devices.[1–5] The high-pressure structural properties of these materials have received renewed interest due to the significant advancements in integrated diamond anvil cell (DAC) techniques and synchrotron radiation as an available light source in experiments. It was shown that, at a moderate pressure, the tetragonal zircon-type compounds with space group $I4_1/amd$ $(Z=4)$ would transform into another tetragonal scheelite phase.[6–13] In this structural phase transition process, coordination anions for A and B cations keep invariable, while the structural symmetry will decline into $I4_1/a$ $(Z=4)$. In addition, experiments indicated that the tetragonal scheelite-type phase also is unstable under high pressure. When pressure further increases, it usually evolves toward a more compacted monoclinic structure concomitant with the increase of coordination number of the B-site cation.[14–22] Detailed descriptions on the interesting high-pressure structural behaviors of the scheelite-type compounds were reported in Ref. 22.

$YCrO_4$ crystallizes into a tetragonal zircon-type lattice at ambient conditions.[23] It consists of the edge-sharing CrO_4 and YO_8 structural units. Along a-axis direction, the larger YO_8 dodecahedra directly connect each other, while they alternately link with the compacted CrO_4 tetrahedra along c-axis direction. The constitution of $YCrO_4$ was described in more detail in Ref. 24. Due to the unusual out-shell electronic configuration $(3d^14s^0)$ of Cr^{5+} ion, magnetic properties were widely studied for $YCrO_4$ as well as for other isostructural $RCrO_4$ series materials,[25–29] where R denotes rare earth elements except for La and Ce. However, no attention has been paid to the high-pressure structural behaviors of these compounds, even though the zircon-type structure is rather sensitive to pressure due to the less compacted constitution.

We present here the high-pressure Raman scattering investigations of $YCrO_4$ in order to explore pressure effects on crystal structure at room temperature. In addition, d-electronic contributions to phase transition pressure (P_c) and Raman vibrations were qualitatively studied.

II. EXPERIMENTAL

High pressure was generated using an improved Mao-Bell-type DAC with 500 μm culets up to 28.9 GPa in this experiment. The highly pure $YCrO_4$ polycrystalline powder synthesized using conventional solid-state reaction method[29] was carefully loaded into a 250 μm stainless-steel gasket hole. The mixture of 4:1 methanol-ethanol was used as pressure transmitting medium to obtain a hydrostatic pressure condition. Pressures were calibrated by ruby luminescence technique.[30,31] Raman spectra were recorded in back-scattering geometry in the frequency region from 100 to 1000 cm^{-1}, using a LABRAM-HR confocal laser Micro-Raman spectrometer (HR800). The 532 nm line of the Verdi-2 solid-state laser was used as a Raman excitation source. A 25× microscope objective lens was applied in order to focus the laser beam and collect the scattered light. The instrument resolution was 1 cm^{-1}. All the measurements were carried out at room temperature.

III. RESULTS AND DISCUSSION

A. Raman spectrum of $YCrO_4$ at ambient conditions

Figures 1(a) and 1(b) show some representative Raman spectra of $YCrO_4$ in the lower-frequency (100–650 cm^{-1}) and higher-frequency (700–1000 cm^{-1}) regions at different pressures, respectively. Group theory analysis[32] predicted that there are twelve Raman active phonon modes $(2A_{1g}+4B_{1g}+B_{2g}+5E_g)$ for the zircon-type compounds in $I4_1/amd$ symmetry (D_{4h}^{19}). In our present experiment, eight Raman active phonon modes are discernable at ambient conditions. According to the assignment methods proposed by Jayaraman *et al.*,[33] six of them can be assigned as the internal vibration modes of CrO_4 tetrahedra: symmetric stretching ν_1 (A_g), antisymmetric stretching ν_3 $(B_g$ and $E_g)$, symmetric bending ν_2 $(A_g$ and $B_g)$, antisymmetric bending ν_4 (B_g); and

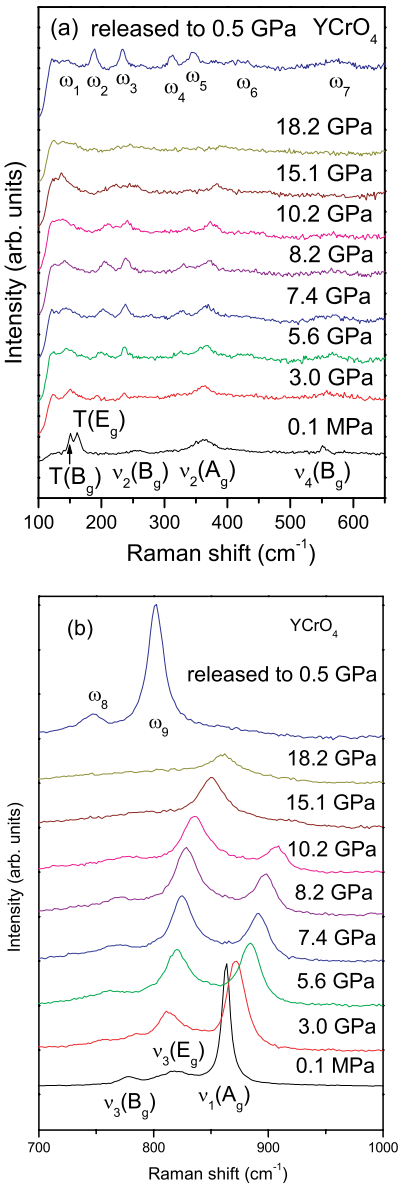

FIG. 1. (Color online) Some representative Raman spectra that show the nonreversible structural transition of $YCrO_4$ at different pressures in (a) 100–650 cm^{-1} and (b) 700–1000 cm^{-1} frequency regions, respectively.

other two are assigned as the external translation modes of CrO_4 units: T (B_g and E_g). Furthermore, the stretching and bending modes reflect the vibrations of Cr-O and O-Cr-O bonds in CrO_4 tetrahedra, respectively.

From the ambient-pressure Raman spectrum as shown in Fig. 1, it is known that the phonon frequencies of the stretching modes are higher than those of other modes. In addition, the intensity of ν_1 (A_g) mode is the strongest and ν_2 (B_g) the weakest. All of these are well in agreement with the general rule of Raman modes of the zircon-type compounds as reported in Ref. 34. However, when compared with many other isostructural compounds such as $CaCrO_4$ and RVO_4 (R=Y, Dy, and Tb),[6,7,12] there is a large increase in the phonon frequency of ν_4 (B_g) mode in $YCrO_4$. This is related to the

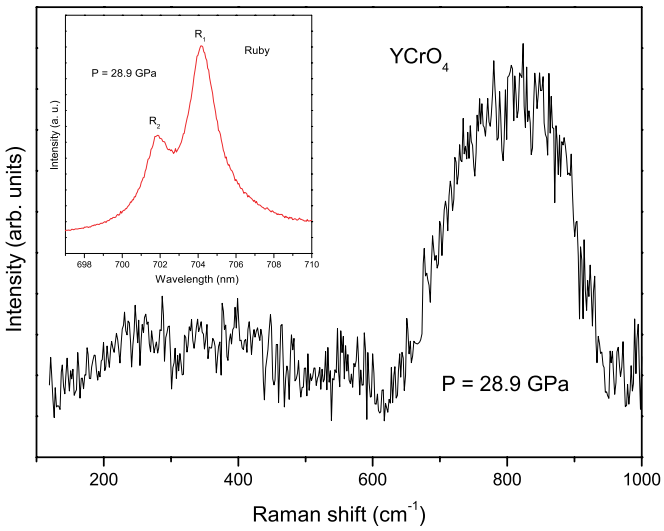

FIG. 2. (Color online) Raman spectrum at the highest pressure 28.9 GPa. The inset shows the ruby luminescence spectrum at this pressure.

effects of $3d^1$ electronic interactions of Cr^{5+} ions as discussed later.

B. Pressure-related Raman spectra

As presented in Fig. 1, the Raman active modes of the zircon-type $YCrO_4$ are rather sensitive to pressure. Just when pressure reaches 3.0 GPa, all the lower-frequency Raman peaks, as well as the ν_3 (E_g) peak have disappeared. In addition, seven new Raman peaks (sign with ω_1, ω_2, ω_3, ω_5, ω_7, ω_8, and ω_9, respectively) are exhibited clearly. These are indicative of structural phase transition in $YCrO_4$. With pressure increasing to 5.6 GPa, two additional new Raman peaks (ω_4 and ω_6) also appear accompanying with the vanish of ν_3 (B_g) mode. However, the intensity of ω_6 and ω_7 Raman peaks decline quickly with pressure due to the pressure-induced broadened effect so that they cannot be identified up to 8.2 GPa. In addition, it is notable that the zircon-phase ν_1 (A_g) vibrational mode always coexists with the new-phase Raman modes in a wider pressure region, and it just becomes ambiguous as pressure increases to 15.1 GPa. At this pressure, the new-phase ω_4 and ω_8 Raman peaks also have become indiscernible, and the ω_2 and ω_3 Raman peaks tend to overlap. Then with pressure up to 18.2 GPa, only the ω_9 Raman peak is observable. To further explore whether there is other possible structural phase transition, pressure is promoted to the highest 28.9 GPa. But only two large humps are observed in the whole phonon frequency region, as shown in Fig. 2. The sharp broadening of Raman peak probably results from pressure-driven structural disordering and/or the reduced hydrostatic pressure condition in DAC. But the ruby luminescence spectrum (see the inset in Fig. 2) shows the obvious separation and the fine symmetry for R_1 and R_2 peaks at 28.9 GPa. Therefore, structural disordering is the main cause for Raman peaks broadening under higher pressure. As a matter of fact, pressure-induced structural disordering or even amorphization is often observed.[35,36]

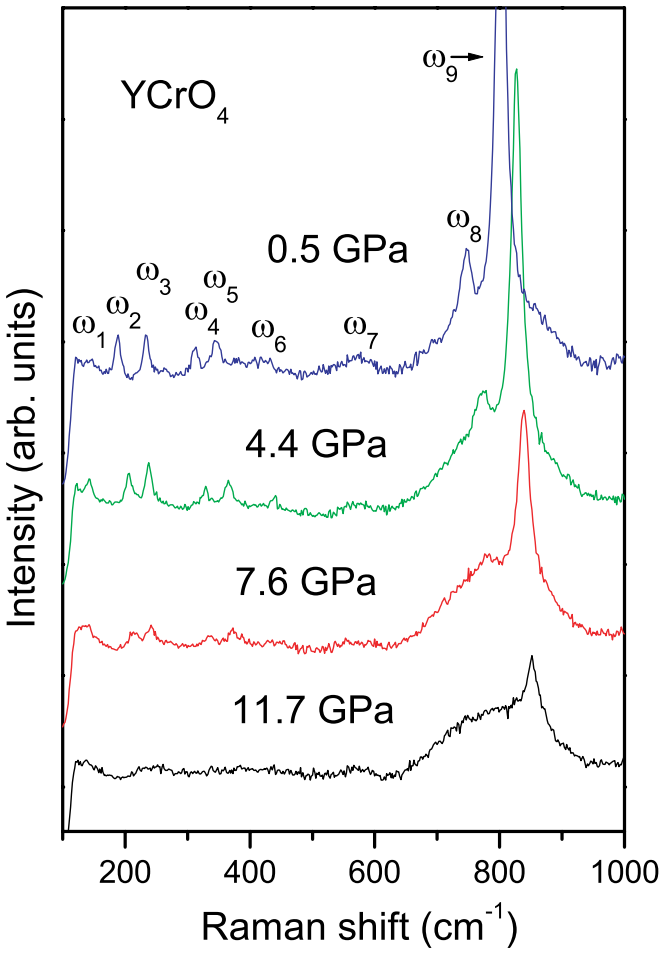

FIG. 3. (Color online) Raman spectra in the decompression process.

Eventually, we gradually released pressure to the lowest 0.5 GPa, and only the new-phase Raman peaks were observed in the whole decompression process as shown in Fig. 3. Accordingly, it is concluded that the structural phase transition occurred at 3.0 GPa is nonreversible. The top pattern in Fig. 1 also presents the pressure-released Raman spectrum to 0.5 GPa in order to demonstrate the nonreversibility for this phase transition.

The pressure dependence of Raman phonon frequencies in the compression process from 0 to 18.2 GPa is shown in Fig. 4. Linear least-square fittings were performed on these data as shown by the solid lines in the figure. The slopes of phonon frequency versus pressure, as well as the ambient-pressure frequencies are listed in Table I. These results are useful to calculate the mode Grüneisen parameters.

C. Zircon to scheelite phase transition in $YCrO_4$

1. Determination of the new phase

Pressure-related Raman spectra have shown that the structural phase transition is sluggish under high pressure in our experimental time scale (staying about 15 min at one pressure). Although this transition has occurred at a lower pressure 3.0 GPa, it will not complete until pressure reaches

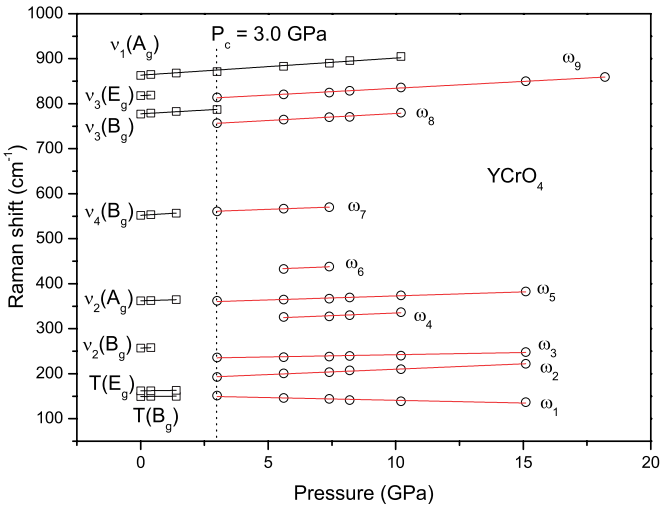

FIG. 4. (Color online) Pressure dependence of phonon frequencies of $YCrO_4$ during compression from 0 to 18.2 GPa. Open squares and circles correspond to the zircon and scheelite phase, respectively. The vertical dotted line presents the observed P_c. Solid lines are linear least-square fittings giving the $d\omega_i/dp$.

15.1 GPa. In order to accelerate the structural transition, it probably is feasible to apply an appropriate temperature during compression. Most recently, we have successfully obtained a bulk $YCrO_4$ sample at moderate temperature and pressure ($P<8$ GPa) (Ref. 24) conditions using a set of cubic anvil apparatus. This sample exhibits a different crystal structure from the zircon-type phase, just like the powder x-ray diffraction patterns shown in Fig. 5. Structural refinement results[24] reveal that it has a tetragonal scheelite-type crystal structure with space group $I4_1/a$. In particular, the scheelite-type $YCrO_4$ shows a similar Raman spectrum with that of the new phase of $YCrO_4$ observed in our Raman scattering experiment, as presented in Fig. 6. Therefore, we can reasonably conclude that the new phase occurred at 3.0 GPa also has a scheelite-type crystal structure in $I4_1/a$ symmetry (C_{4h}^6). Actually, a large number of available experimental data also support the fact that the zircon-type phase seemingly always transforms into a nonreversible scheelite phase at an appropriate pressure.[6–13]

2. Mode Grüneisen parameters for both phases

Table I lists the ambient-pressure phonon frequencies ω_{0i}, their pressure derivatives $d\omega_i/dp$ and mode Grüneisen parameters γ_i for both phases of $YCrO_4$. It is known that the Cr-O bond stretching modes exhibit the larger Raman shift with pressure. In addition, the ω_1 mode of the scheelite phase shows a negative pressure derivative. The mode Grüneisen parameters were calculated using the formula: $\gamma_i = (B_0/\omega_{0i})(d\omega_i/dp)$, where B_0 and ω_{0i} are the bulk modulus and the ambient-pressure phonon frequencies, respectively. The $d\omega_i/d_p$ and the scheelite-phase ω_{0i} come from the linear fitting results as described above. Errandonea *et al.* have recently put forward an experiential criterion: $B_0(\mathrm{GPa}) = (610 \pm 110) Z_A/d_{A\text{-}O}^3$ to calculate the scheelite-phase bulk modulus,[22] where Z_A is the formal charge for A-site cation,

TABLE I. The ambient-pressure phonon frequencies ω_{0i}, pressure derivatives of frequencies $d\omega_i/dp$, and mode Grüneisen parameters γ_i for various Raman modes of the zircon- and scheelite-type $YCrO_4$.

Zircon phase				Scheelite phase			
Raman mode	ω_{0i} (cm^{-1})	$d\omega_i/dp$ ($cm^{-1}GPa^{-1}$)	γ_i	Raman mode	ω_{0i} (cm^{-1})	$d\omega_i/dp$ ($cm^{-1}GPa^{-1}$)	γ_i
T (B_g)	149	0.6	0.38	ω_1	153	−1.2	−1.09
T (E_g)	162	0.71	0.42	ω_2	186	2.4	1.79
ν_2 (B_g)	257	2.0	0.74	ω_3	232	1.1	0.66
ν_2 (A_g)	362	1.8	0.47	ω_4	312	2.3	1.02
ν_4 (B_g)	552	3.6	0.62	ω_5	355	1.8	0.70
ν_3 (B_g)	778	4.2	0.51	ω_6	421	2.3	0.76
ν_3 (E_g)	818	4.0	0.46	ω_7	555	2.1	0.53
ν_1 (A_g)	863	4.6	0.51	ω_8	747	3.1	0.58
				ω_9	804	3.0	0.52

and $d_{A\text{-}O}$ is the average A-O distance (in Å) in AO_8 units. Consequently, the bulk modulus of the scheelite-type $YCrO_4$ can be estimated to be 139 GPa (the $d_{Y\text{-}O}$ used here was determined to be 2.37 Å based on the refinement results[24]). Kusaba *et al.*[9] analyzed the mechanism of structural phase transition from zircon to scheelite and proposed that the density would increase by about 10% when this transition happened under high pressure. In addition, it was reported that the bulk modulus and the density obey the following relationship: $B_{02}/B_{01}=(\rho_{02}/\rho_{01})^4$ in the zircon-scheelite phase transition (B and ρ denote the bulk modulus and the density, and the subscripts 1 and 2 present the zircon and scheelite phase, respectively).[39,40] Therefore, the bulk modulus of the zircon-type $YCrO_4$ could be calculated to be 95 GPa, and the corresponding mode Grüneisen parameters also were obtained, as shown in Table I.

Due to the changes of bond lengths in the zircon-scheelite transition in ABO_4 compounds, Raman phonon frequencies of the B-O stretching modes usually will decrease, as reported in Refs. 6, 7, 10, and 12. As far as $YCrO_4$ is concerned, the ambient-pressure phonon frequency of ν_1 (A_g) vibrational mode declines from 863 cm^{-1} to 804 cm^{-1} as listed in Table I. According to the expression of force constant κ: $\nu=1/2\pi\sqrt{\kappa/m}$ (ν and m denote phonon frequency and atomic renormalized mass, respectively), the Cr-O bond strength will decrease by about 3.5%. It implies that the Cr-O bond lengths in CrO_4 units will increase, and the density of the CrO_4 polyhedra probably will decline when phase transition happens. Therefore, we think that the increase of density in the zircon-scheelite transition in $YCrO_4$ does not directly result from the reduction of coordination polyhedra, but from their more efficient packing as well as the elimination of structural voids among polyhedra, just as Reid *et al.* reported on the prototype of the zircon $ZrSiO_4$.[37]

3. *Effects of 3d electrons on P_c and Raman vibrations*

Table II lists a series of physical parameters, such as phase transition pressure P_c, ionic radii,[38] and so on for some

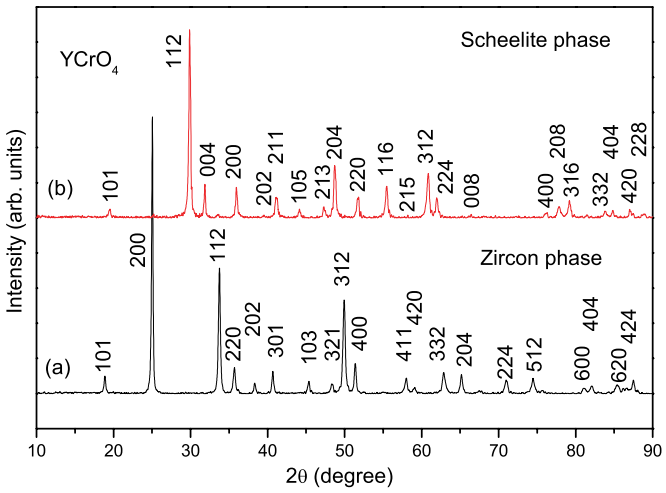

FIG. 5. (Color online) X-ray powder diffraction patterns and the corresponding indices for the zircon- and scheelite-type $YCrO_4$.

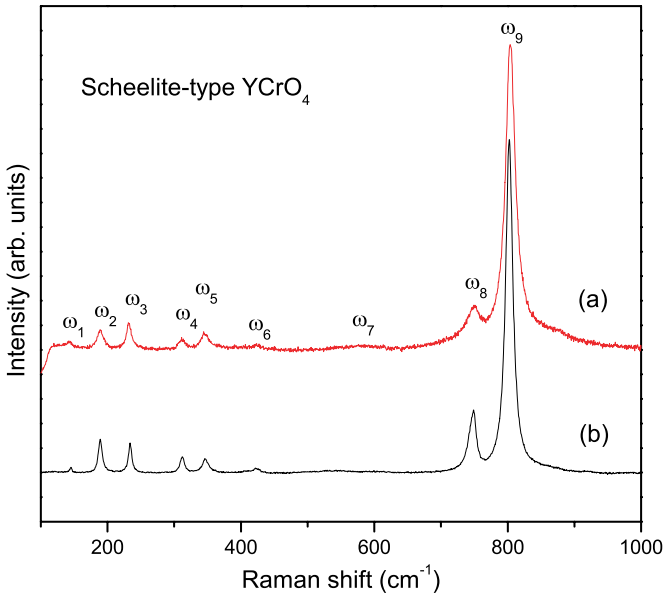

FIG. 6. (Color online) Raman spectra of (a) the pressure-released $YCrO_4$ to 0.5 GPa and (b) the scheelite-type $YCrO_4$ prepared using moderate temperature and pressure conditions.

TABLE II. Phase transition pressure P_c, the radii of A-site cation and BO_4 units and their ratios, phonon frequencies of ν_4 (B_g) mode for a series of ABO_4 zircon-type compounds.

ABO_4 type Compound	P_c (GPa)	R_A[a] (Å)	R_{BO_4}[a] (Å)	R_{BO_4}/R_A	ν_4 (B_g) (cm^{-1})	Reference
$CaCrO_4$	6.0	1.12	1.66	1.48	464	12
$YCrO_4$	3.0	1.019	1.745	1.712	552	this work
YVO_4	7.5/8.5	1.019	1.755	1.722	487	6 and 8
$DyVO_4$	6.5±0.3	1.027	1.755	1.709	482	7
$TbVO_4$	6.6±0.6	1.040	1.755	1.688	480	7
$ZrSiO_4$	19.7/23±1	0.84	1.66	1.98	—	11 and 10

[a]Reference 38.

available data of ABO_4 zircon-type compounds at room temperature. Due to the smaller A-site cation radius as well as the more compacted BO_4 coordination polyhedra, the $A^{4+}B^{4+}O_4$-type $ZrSiO_4$ displays the highest phase transition pressure. In addition, this type of compound usually has a larger bulk modulus, and potentially can be used as a kind of superhard materials.[39] For $A^{3+}B^{5+}O_4$- and $A^{2+}B^{6+}O_4$-type compounds, it was reported that P_c would increase with the increase of the ratio R_{BO_4}/R_A, where R_{BO_4} and R_A present the radii of BO_4 units and A-site cation.[41] R_{BO_4} were calculated according to the plus rule $R_{BO_4}=R_B+R_O$ using Shannon's ionic radii (R_O was set to be 1.40 Å).[38] The values of R_A, R_{BO_4} and R_{BO_4}/R_A for different compounds are shown in Table II. It is known that only $YCrO_4$ deviates from the criterion mentioned above. Unlike other compounds listed in Table II with inert-element-like B-site cation configuration, there is a $3d^1$ electron in the out shell of Cr^{5+} ion in $YCrO_4$. During the compression, the cooperative interactions of these electrons will influence the system energy. As a result, the phase transition pressure of $YCrO_4$ is no more consistent with the criterion. In our views, P_C is related to both ionic radius and electronic configuration in the zircon-type compounds.

In addition, Raman scattering experiments showed that aside from the Cr-O bond stretching modes, the phonon frequencies of other modes usually do not exceed 500 cm^{-1} in ABO_4 zircon-type compounds as presented in Table II. However, $YCrO_4$ exhibits unusual Raman vibrations. As a specific example, the frequency of the bending mode ν_4 (B_g) reaches to 552 cm^{-1}. We believe that the unusual Raman vibrations in $YCrO_4$ also are related to the effects of $3d^1$ electrons. The interactions of d electrons will influence the bond lengths and angles in CrO_4 polyhedra. Thereby it results in the unusual Raman behaviors of $YCrO_4$.

IV. CONCLUSION

The high-pressure Raman scattering was performed on the zircon-type $YCrO_4$ in 0–28.9 GPa at ambient temperature. The crystal structure of this compound sensitively depends on pressure. When pressure increases to 3.0 GPa, the tetragonal zircon phase will evolve toward a new phase. However this phase transition cannot complete until 15.1 GPa. The pressure-released Raman spectra show that the high-pressure new phase is quenchable to ambient conditions. Based on the similar Raman spectra, we assigned the new phase to be the same structure with our scheelite-type $YCrO_4$ in $I4_1/a$ symmetry prepared at moderate temperature and pressure conditions. The mode Grüneisen parameters were calculated according to the fitting results and the experiential criterion for bulk moduli. The cooperative interactions of d electrons in Cr^{5+} ions will influence the system energy and the bond lengths and angles of CrO_4 tetrahedra. These are responsible for the unusual P_c and Raman vibrations observed in $YCrO_4$.

ACKNOWLEDGMENTS

This work was supported by the NSF and the Ministry of Science and Technology of China through Research Projects No. 2002CB613301, No. 2005CB724402, No. 50321101, No. 50332020, and No. 50371099.

*Corresponding author. Email address: Jin@aphy.iphy.ac.cn

[1] M. Ishii and M. Kobayashi, Prog. Cryst. Growth Charact. Mater. **23**, 245 (1991).
[2] N. Faure, C. Borel, M. Couchaud, G. Basset, R. Templier, and C. Wyon, Appl. Phys. B: Lasers Opt. **63**, 593 (1996).
[3] M. G. Jani, F. L. Naranjo, N. P. Barnes, K. E. Murray, and G. E. Lockard, Opt. Lett. **20**, 8 (1995).
[4] M. Kobayashi, M. Ishi, Y. Usuki, and H. Yahagi, Nucl. Instrum. Methods Phys. Res. A **333**, 429 (1993).
[5] M. Nikl, P. Bohacek, N. Mihokova, N. Solovieva, A. Vedda, M. Martini, G. P. Pazzi, P. Fabeni, M. Kobayashi, and M. Ishii, J. Appl. Phys. **91**, 5041 (2002).
[6] A. Jayaraman, G. A. Kourouklis, G. P. Espinosa, A. S. Cooper, and L. G. Van Uitert, J. Phys. Chem. Solids **48**, 755 (1987).
[7] S. J. Duclos, A. Jayaraman, G. A. Kourouklis, A. S. Cooper, and R. G. Maines, J. Phys. Chem. Solids **50**, 769 (1989).

[8] X. Wang, I. Loa, K. Syassen, M. Hanfland, and B. Ferrand, Phys. Rev. B **70**, 064109 (2004).
[9] K. Kusaba, T. Yagi, M. Kikuchi, and Y. Syono, J. Phys. Chem. Solids **47**, 675 (1986).
[10] E. Knittle and Q. Williams, Am. Mineral. **78**, 245 (1993).
[11] W. Van Westrenen, M. R. Frank, J. M. Hanchar, Y. Fei, R. J. Finch, and C. S. Zha, Am. Mineral. **89**, 197 (2004).
[12] Y. W. Long, W. W. Zhang, L. X. Yang, Y. Yu, R. C. Yu, S. Ding, Y. L. Liu, and C. Q. Jin, Appl. Phys. Lett. **87**, 181901 (2005).
[13] Y. W. Long, L. X. Yang, S. J. You, Y. Yu, R. C. Yu, C. Q. Jin, and J. Liu, J. Phys.: Condens. Matter **18**, 2421 (2006).
[14] W. I. F. David and A. M. Glazer, Phase Transitions **1**, 155 (1979).
[15] L. E. Depero and L. Sangaletti, J. Solid State Chem. **129**, 82 (1997).
[16] A. Grzechnik, K. Syassen, I. Loa, M. Hanfland, and J. Y. Gesland, Phys. Rev. B **65**, 104102 (2002).
[17] S. R. Shieh, L. C. Ming, and A. Jayaraman, J. Phys. Chem. Solids **57**, 205 (1996).
[18] A. Sen, S. L. Chaplot, and R. Mittal, J. Phys.: Condens. Matter **14**, 975 (2002); Phys. Rev. B **68**, 134105 (2003).
[19] A. Grzechnik, W. A. Crichton, M. Hanfland, and S. Van Smaalen, J. Phys.: Condens. Matter **15**, 7261 (2003).
[20] S. Li, R. Ahuja, Y. Wang, and B. Johansson, High Press. Res. **23**, 343 (2003).
[21] V. Panchal, N. Garg, A. K. Chauhan, B. Sangeeta, and S. M. Sharma, Solid State Commun. **130**, 203 (2004).
[22] D. Errandonea, J. Pellicer-Porres, F. J. Manjón, A. Segura, C. Ferrer-Roca, R. S. Kumar, O. Tschauner, P. Rodriquez-Hernández, J. Lopez-Solano, S. Radescu, A. Mújica, A. Muñoz, and G. Aquilanti, Phys. Rev. B **72**, 174106 (2005).
[23] V. H. Schwarz, Z. Anorg. Allg. Chem. **332**, 137 (1963).
[24] Y. W. Long *et al.* (unpublished).
[25] E. Jimenez, J. Isasi, and R. S. Puche, J. Solid State Chem. **164**, 313 (2002); J. Alloys Compd. **312**, 53 (2000).
[26] R. S. Puche, E. Jimenez, J. Isasi, M. T. F. Diaz, and J. L. G. Munoz, J. Solid State Chem. **171**, 161 (2003).
[27] K. Tezuka and Y. Hinatsu, J. Solid State Chem. **160**, 326 (2001).
[28] E. Jimenez, P. Bonville, J. A. Hodges, P. C. M. Gubbens, J. Isasi, and R. S. Puche, J. Magn. Magn. Mater. **272**, 571 (2004).
[29] E. J. Melero, N. H. van Dijk, W. H. Kraan, P. C. M. Gubbens, J. Isasi, and R. S. Puche, J. Magn. Magn. Mater. **288**, 1 (2005).
[30] G. J. Piermarini, S. Block, J. D. Barnett, and R. A. Forman, J. Appl. Phys. **46**, 2774 (1975).
[31] H. K. Mao, J. Xu, and P. M. Bell, J. Geophys. Res. **91**, 4673 (1986).
[32] S. A. Miller, H. H. Caspers, and H. E. Rast, Phys. Rev. **168**, 964 (1968).
[33] A. Jayaraman, B. Batlogg, and L. G. Van Uitert, Phys. Rev. B **28**, 4774 (1983).
[34] A. Muller, E. J. Baran, and R. O. Carer, Struct. Bonding (Berlin) **26**, 81 (1976).
[35] S. K. Deb, M. Wilding, M. Somayazulu, and P. F. McMillan, Nature **414**, 528 (2001).
[36] D. Errandonea, M. Somayazulu, and D. Häusermann, Phys. Status Solidi B **235**, 162 (2003).
[37] A. F. Reid and A. E. Ringwood, Earth Planet. Sci. Lett. **6**, 205 (1969).
[38] R. D. Shannon, Acta Crystallogr., Sect. A: Cryst. Phys., Diffr., Theor. Gen. Crystallogr. **32**, 751 (1976).
[39] H. P. Scott, Q. Williams, and E. Knittle, Phys. Rev. Lett. **88**, 015506 (2002).
[40] D. L. Anderson, Geophys. J. R. Astron. Soc. **13**, 9 (1967).
[41] D. Errandonea, F. J. Manjon, M. Somayazulu, and D. Hausermann, J. Solid State Chem. **177**, 1087 (2004).